JACS
JOURNAL OF THE AMERICAN CHEMICAL SOCIETY
pubs.acs.org/JACS
Article

Revealing the Orientation Selectivity of Tetrapyridyl-Substituted Porphyrins Constrained in Molecular "Klotski Puzzles"

Zewei Yi, Yuan Guo, Rujia Hou, Zhaoyu Zhang, Yuhong Gao, Chi Zhang,* and Wei Xu*

Cite This: J. Am. Chem. Soc. 2023, 145, 22366−22373

ABSTRACT: Understanding and controlling molecular orientations in self-assembled organic nanostructures are crucial to the development of advanced functional nanodevices. Scanning tunneling microscopy (STM) provides a powerful toolbox to recognize molecular orientations and to induce orientation changes on surfaces at the single-molecule level. Enormous effort has been devoted to directly controlling the molecular orientations of isolated single molecules in free space. However, revealing and further controlling molecular orientation selectivity in constrained environments remain elusive. In this study, by a combination of STM imaging/manipulations and density functional theory calculations, we report the orientation selectivity of tetrapyridyl-substituted porphyrins in response to various local molecular environments in artificially constructed molecular "Klotski puzzles" on Au(111). With the assistance of STM lateral manipulations, "sliding-block" molecules were able to enter predefined positions, and specific molecular orientations were adopted to fit the local molecular environments, in which the intermolecular interaction was revealed to be the key to achieving the eventual molecular orientation selectivity. Our results demonstrate the essential role of local molecular environments in directing single-molecule orientations, which would shed light on the design of molecular structures to control preferred orientations for further applications in molecular nanodevices.

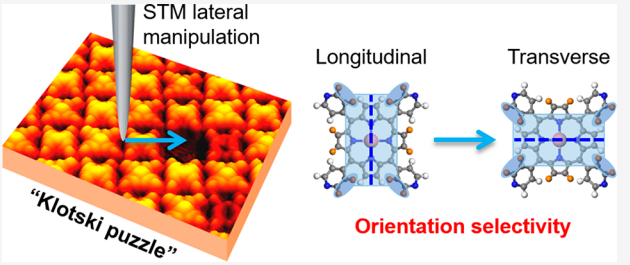

INTRODUCTION

Molecular self-assembly is flourishing with the growing importance of organic-based nanomaterials. Recognizing and controlling molecular orientations in self-assembled organic nanostructures at the single-molecule level is essential for both the in-depth understanding of the self-assembly mechanism and the development of advanced functional nanodevices. Specifically, molecular orientation has proven to be crucial in influencing and determining the electrical and optical properties of organic semiconductors.[1−4] Many factors, such as molecular weight, blending, and melt annealing, have been tuned to induce the global orientation change in organic films to achieve the ideal device performance.[4] In addition, conventional spectroscopic methods, such as ellipsometry[1] and X-ray-based techniques,[2,3] have been extensively used to monitor the average molecular orientations, allowing the discrimination between horizontal (lying-down) and vertical (standing-up) orientations, while leaving the specific molecular orientations in the plane elusive. Advances in the surface science techniques, such as scanning probe microscopy (SPM), provide great opportunities to directly visualize the orientation heterogeneity of organic molecules on surfaces at the single-molecule level.[5−11] Furthermore, SPM manipulations provide a versatile toolbox to induce molecular motions and reactions,[12−14] including translation[15−18] and rotation.[16−22] Accordingly, molecular orientation changes have been directly triggered and controlled by SPM manipulations on the target molecules in free space.[16−22] However, molecular orientation selectivity in constrained environments remains elusive.[17,23] Therefore, it is of general interest to artificially construct various local environments to explore the influence of peripheral intermolecular interactions on the orientation selectivity of target molecules, which would shed light on the fundamental understanding of orientation selectivity at the single-molecule level and benefit the further development of advanced functional organic nanodevices.

In this study, the tetrapyridyl-porphyrin (H_2TPyP)-based molecules were used as the building blocks (cf. Scheme 1). Due to the intramolecular steric hindrance, the H_2TPyP-based molecules (both intact and metalated ones) adopt a saddle-shaped adsorption geometry[24,25] on Au(111), leading to the apparently rectangular morphology in the STM images (Scheme 1). Accordingly, the molecular orientations can be intuitively recognized based on the direction of the long axis of rectangles (as depicted by the blue dashed lines). To explore the orientation selectivity of H_2TPyP-based molecules in

Received: April 12, 2023
Published: September 28, 2023

https://doi.org/10.1021/jacs.3c03777
J. Am. Chem. Soc. 2023, 145, 22366−22373

Scheme 1. Overview of the Molecular Orientation Selectivity in a "Klotski Puzzle"[a]

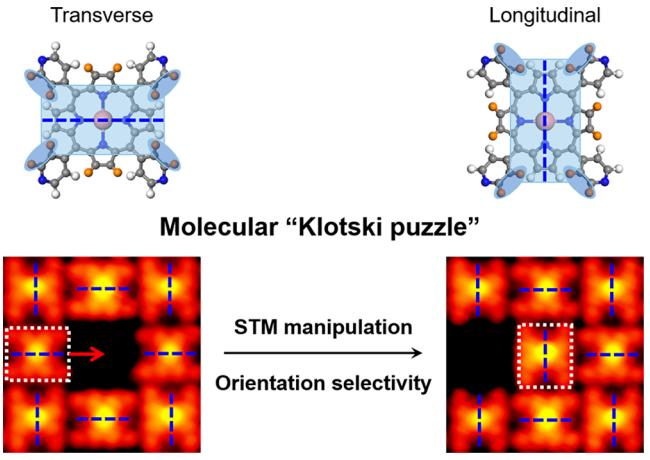

[a]Top: Optimized structural models of the Na-based tetrapyridyl-substituted porphyrin molecule on Au(111) with two orthogonal orientations, i.e., transverse and longitudinal, respectively, where the underlying substrates are omitted for clarity. The corresponding STM morphologies with prominent apparent height are shaded blue, and the apparent long axes are indicated by blue dashed lines. C: gray; N: blue; Na cluster: pink. Hydrogen atoms above and below the molecular plane are colored orange and white, respectively. Bottom: STM images recorded at the same region showing the "parking" process of the target "sliding-block" molecule (as depicted by the white dashed rectangles in the left and right panels, respectively) in a molecular "Klotski puzzle" triggered by the STM lateral manipulation (the direction is indicated by a red arrow), in which the molecular orientation has to change orthogonally to fit the local molecular environment. Scanning conditions: V_t = −1.4 V, and I_t = 0.7 nA.

constrained environments, we fabricated a close-packed self-assembled chessboard structure with some naturally existing vacancies by co-deposition of H_2TPyP molecules and sodium chloride (NaCl) onto Au(111),[25,26] in which H_2TPyP-based molecules are aligned alternately with two orthogonal orientations (i.e., transverse and longitudinal). Interestingly, based on STM lateral manipulations,[27,28] various molecular patterns with different cavities, figuratively, the molecular "Klotski puzzles", were artificially constructed by collecting dispersed vacancies, thus providing the possibility to investigate the orientation selectivity of H_2TPyP-based molecules in constrained environments (Scheme 1).

Herein, we reveal that the orientation selectivity of the constrained H_2TPyP-based molecules is determined by the local molecular environments. When manipulating the "sliding-block" molecules in "Klotski puzzles", as long as at least one side of a target molecule interacts with an adjacent molecule, it must adopt a specific orientation (i.e., either transverse or longitudinal) to fit the local environment while maintaining the orthogonally alternate orientations with respect to the neighbors. For molecules without constraint, i.e., no neighbors on any side, interestingly, no orientation selectivity was observed, and transverse and longitudinal orientations were found to interconvert during scanning at room temperature (RT, ~300 K). Furthermore, density functional theory (DFT) calculations validated that the orientation selectivity of molecules constrained in the "Klotski puzzles" was driven by the intermolecular packing in energetically more favorable manners, and two possible pathways (i.e., molecular rotation and conformational change) to achieve the orientation change were proposed. Our results reveal the selectivity of molecular orientations in constrained nanostructures via local intermolecular interactions at the single-molecule level, which is a step forward in understanding and further controlling molecular orientations in self-assembled organic nanostructures.

RESULTS AND DISCUSSION

Deposition of H_2TPyP molecules and NaCl onto Au(111) followed by annealing at ~510 K or above led to the formation of a close-packed chessboard structure dominantly composed of metalated Na_5TPyP molecules.[25] The chessboard structure is stabilized mainly by the electrostatic interactions between the peripheral pyridyl groups of H_2TPyP-based molecules and Na derived from NaCl.[25,26,29,30] In addition, with a slightly higher annealing temperature (of around 520−530 K), several dispersed cavities (with single molecules missing) naturally existed in the molecular island (cf. Figure S1). It thus provides an ideal template for further artificial construction of various local molecular environments, i.e., molecular "Klotski puzzles", allowing us to explore the influence of local environments on the orientation selectivity of target "sliding-block" molecules. To investigate the molecular orientation selectivity in constrained environments at the single-molecule level, a series of STM lateral manipulations were conducted in a line-scan mode[27,28] (see Methods in the Supporting Information). As shown in the high-resolution STM image (Figure 1a), the target "sliding-block" molecule A was first manipulated along the direction of the red arrow toward the upper cavity. Interestingly, it successfully entered the cavity, and the molecular orientation changed orthogonally, with the molecule appearing as A′ (Figure 1b). Next, manipulations on molecules B and C resulted in the same phenomena, as shown in Figure 1b−d. Such an accompanying molecular orientation change within "Klotski puzzles" is also applicable to other saddle-shaped tetrapyridyl-substituted porphyrins, including the intact H_2TPyP and another metalated form (Na_2TPyP) in our study (Figure S2), and the manipulated molecules are stable after movements (Figure S3).

To understand the orientation selectivity in a more general case, we intentionally constructed cavities in different shapes by gradually moving the surrounding molecules away via STM lateral manipulations and collecting the dispersed vacancies. Such highly reliable STM lateral manipulations also show promising applications in the construction of tailored nanopatterns on surfaces.[18,31,32] As a result, the cavity consisting of three vacancies was constructed with the target "sliding-block" molecule D located at the top right of the cavity, which provided a template to explore the molecular orientation selectivity in a 2 × 2 cavity (Figure 1e). By successively moving the molecule D to the adjacent positions, it underwent continuous orientation changes after each movement within the "Klotski puzzles" (Figure 1e−h). Besides, a larger cavity with eight vacancies was delicately constructed to further enlarge the free space for the target molecule, and the "sliding-block" molecule E was initially positioned at the corner of the 3 × 3 cavity (Figure 1i). STM lateral manipulations were repeatedly performed on molecule E to induce the movements in the directions of the red arrows (Figure 1i−l). Interestingly, after the manipulations, the target molecule was observed to move a two-molecule distance each time and unexceptionally adopt the original orientation at the destinations. It is noteworthy that the sizes of both the 2 × 2 and 3 × 3 cavities are large enough to host the target molecule in any orientation,

https://doi.org/10.1021/jacs.3c03777
J. Am. Chem. Soc. 2023, 145, 22366−22373

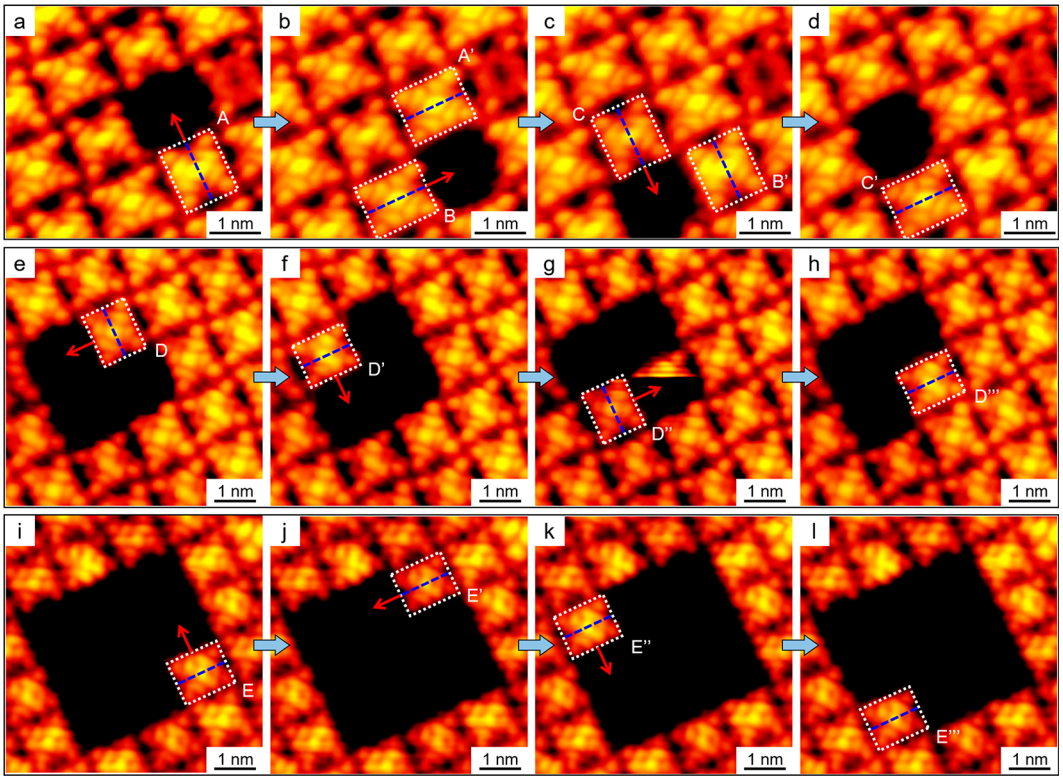

Figure 1. Molecular orientation selectivity in single-cavity and 2D-cavity "Klotski puzzles". (a–d) STM images recorded at the same region showing that the target "sliding-block" molecules were manipulated to the adjacent 1 × 1 cavity, accompanied by orientation changes. The three target "sliding-block" molecules before and after manipulations were labeled A, B, C, and A′, B′, C′, respectively. (e–h) STM images showing the successive manipulations on the target "sliding-block" molecule D in a 2 × 2 cavity, accompanied by orientation changes. (i–l) STM images showing the successive manipulations on the target "sliding-block" molecule E in a 3 × 3 cavity, where the target molecule adopted the original orientation to fit the local environment after moving a two-molecule distance. Scanning conditions: V_t = −1.2 V, and I_t = 0.6–0.7 nA.

and therefore, the factor of spatial constraint should not be the reason for the orientation change.

To further reveal the orientation changes in relation to the displacement steps, linear 1D-channel "Klotski puzzles" were constructed. As shown in Figure 2a,b, the STM manipulation on the "sliding-block" molecule A along the channel resulted in the movement of a two-molecule distance (from A to A′), where the target molecule adopted the original orientation at the destination. Then, when the molecules B and C were manipulated along the channels to move a three-molecule distance (from B to B′ shown in Figure 2c,d) or a five-molecule distance (from C to C′ shown in Figure 2e,f), the target molecules changed their orientations. Therefore, when a "sliding-block" molecule is moved for a distance with odd times of a single-molecule length in the channel, its orientation has to change orthogonally (by undergoing odd times of orientation changes). On the contrary, when it is moved for a distance with even times of a single-molecule length in the channel, it adopts the original orientation (by undergoing even times of orientation changes). Thus, whether the molecular orientations change in the "Klotski puzzles" is not determined by STM manipulations.

Instead, the local molecular environment is the key to the orientation selectivity; that is, a specific orientation (either transverse or longitudinal) has to be adopted to keep the orthogonally alternate orientations with respect to the neighbors. As shown above in Figure 1a–d, after the manipulations, the target "sliding-block" molecules were always constrained by three adjacent molecules (also see Figure S4a), indicating that the molecular orientation can be controlled by a three-sided constraint. Moreover, when the constraint was reduced to two-sided, as shown in Figure 1e–h and i–l, such a constraint was also valid to determine the molecular orientations (also see Figure S4b). Then, a question arises: how about the one-sided constraint?

Thereafter, we tried to construct more complicated "Klotski puzzles" to produce scenarios of one-sided constraint. As shown in Figure 3a,b, the target "sliding-block" molecule A was initially constrained on three sides and was then manipulated downward to the adjacent cavity, where only a one-sided constraint was available. Interestingly, it was observed that the molecular orientation also changed orthogonally (with the molecule appearing as A′) to fit its interacting neighbor. In addition, in a larger cavity, another target "sliding-block" molecule B was manipulated downward for a two-molecule distance to reach the position constrained on only one side, and the orientation of molecule B′ also fitted its interacting neighbor (Figure 3c,d). Similarly, molecules initially constrained on one side also obeyed the rule (Figure S5). Therefore, it turned out that the constraint from an adjacent molecule interacting only on one side is strong enough to force a target molecule to follow the rule of orientation selectivity.

To further explore the influence of the local molecular environments and to test the extremes of constraint even down to zero-sided, a porous nanostructure template[30] (Figure 4) formed by intact H_2TPyP molecules and Na was applied, where some molecules without constraint (i.e., no neighbors interacting on any side) are depicted by blue rectangles, e.g.,

https://doi.org/10.1021/jacs.3c03777
J. Am. Chem. Soc. 2023, 145, 22366–22373

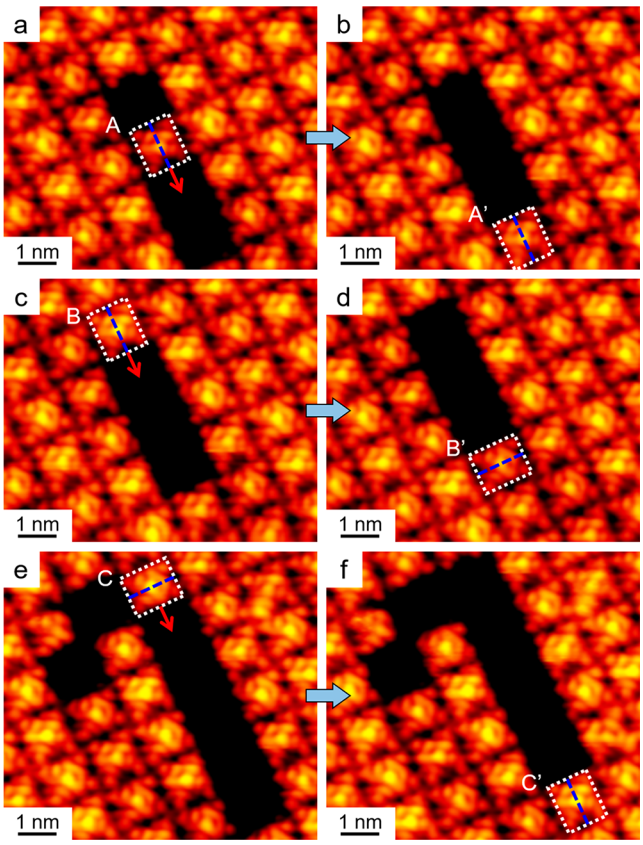

Figure 2. Molecular orientation selectivity in 1D-channel "Klotski puzzles". STM images showing the manipulations on the target "sliding-block" molecules along the 1D channels, in which (a, b) the target molecule adopted the original orientation after moving a two-molecule distance (from A to A′); (c–f) the target molecules changed the orientations after moving (c, d) a three-molecule distance (from B to B′) or (e, f) a five-molecule distance (from C to C′). Scanning conditions: V_t = −1.2 V, and I_t = 0.6–0.7 nA.

molecules A, B, C, and D. Due to the absence of steric hindrance from the adjacent molecules, the rule of orientation selectivity is not valid for these molecules anymore, and interestingly, the orientations (i.e., transverse and longitudinal) of molecules A, B, C, and D were found to interconvert during scanning at RT (Figure 4a–d). Notably, the orientation of a given molecule without any constraint initially can be well controlled by moving another one next to it (forming a one-sided constraint) and is then strictly determined by the orientation of the adjacent molecule, following the rule of orthogonally alternate orientation (see Figure S6 for more details). Additionally, the unconstrained Na_5TPyP molecule was also observed to change the orientations *in situ* without selectivity (Figure S7). Furthermore, DFT calculations were performed to verify the orientation changes in such a porous nanostructure. As shown in Figure 4e, DFT-optimized structural models of the networks containing the target molecules (shaded blue) with the two orientations on Au(111) were calculated to have almost the same potential energy, and thus, it is reasonable for these two orientations to interconvert as observed experimentally. The corresponding enlarged STM images with respect to the models are shown in Figure S8.

To elucidate the underlying mechanism involved in the orientation selectivity in the "Klotski puzzles" as shown above,

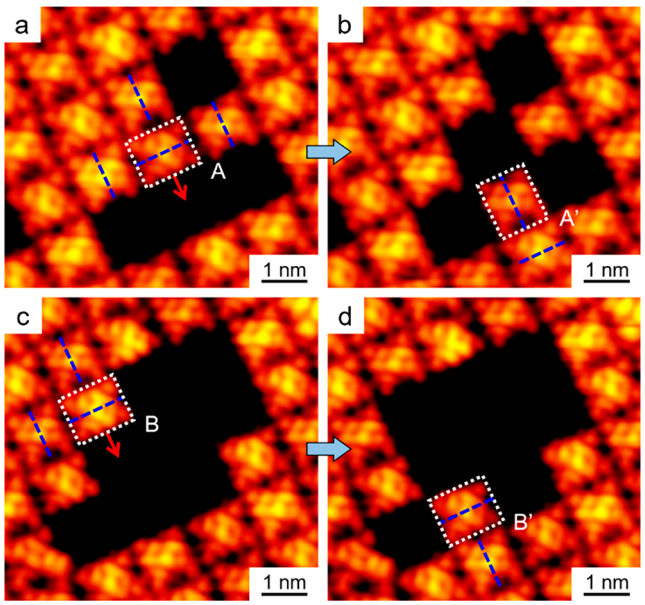

Figure 3. Molecular orientation selectivity in more complicated "Klotski puzzles". (a, b) STM images showing the manipulation on the target "sliding-block" molecule (from A to A′), where only one side of the target molecule interacted with a neighboring molecule after the manipulation, and the target molecule changed the orientation to fit the local environment. (c, d) Manipulation on another target molecule (from B to B′) with only one side interacting with a neighboring molecule at the destination, where the target molecule adopted the original orientation after moving a two-molecule distance. The apparent long axes of the molecules directly interacting with the target molecules are highlighted by blue dashed lines. Scanning conditions: V_t = −1.2 V, and I_t = 0.6–0.7 nA.

DFT calculations were performed. The first question is why the orientation selectivity is valid in the "Klotski puzzles". Figure S9a–c show the situations of moving the target molecule to the position constrained by three-sided molecules. The molecular network structures before and after the manipulation with an orientation change were calculated to have an identical potential energy (see the red stars in Figure S9c). On the contrary, when the orientation of the target molecule is maintained during the "parking" process, the single-point calculated potential energies (blue dots) increase drastically as the molecule moves away from the initial position and remain at a high level during the approach, indicating a much lower stability in this case compared to the situation with an orientation change involved at the destination. Moreover, when the "sliding-block" molecules are moved to positions with two-sided (Figure S9d–f) or one-sided constraints (Figure S9g–i), respectively, similar situations are obtained with respect to the changes in potential energies. Therefore, as long as at least one side of the target molecule interacts with a neighboring molecule, the orthogonally alternate orientation has to be adopted to fit the local molecular environment, forming the energetically more favorable structure.

Moreover, another critical question is how the orientation change occurs. Two possible pathways were proposed, i.e., molecular rotation and conformational change (Figure 5a). The corresponding pathways and energy barriers were calculated for two different situations, where there is (i) sufficient or (ii) constrained space for a target molecule, to interpret the cases of molecules located in a large cavity or in a 1D channel, respectively.

https://doi.org/10.1021/jacs.3c03777
J. Am. Chem. Soc. 2023, 145, 22366–22373

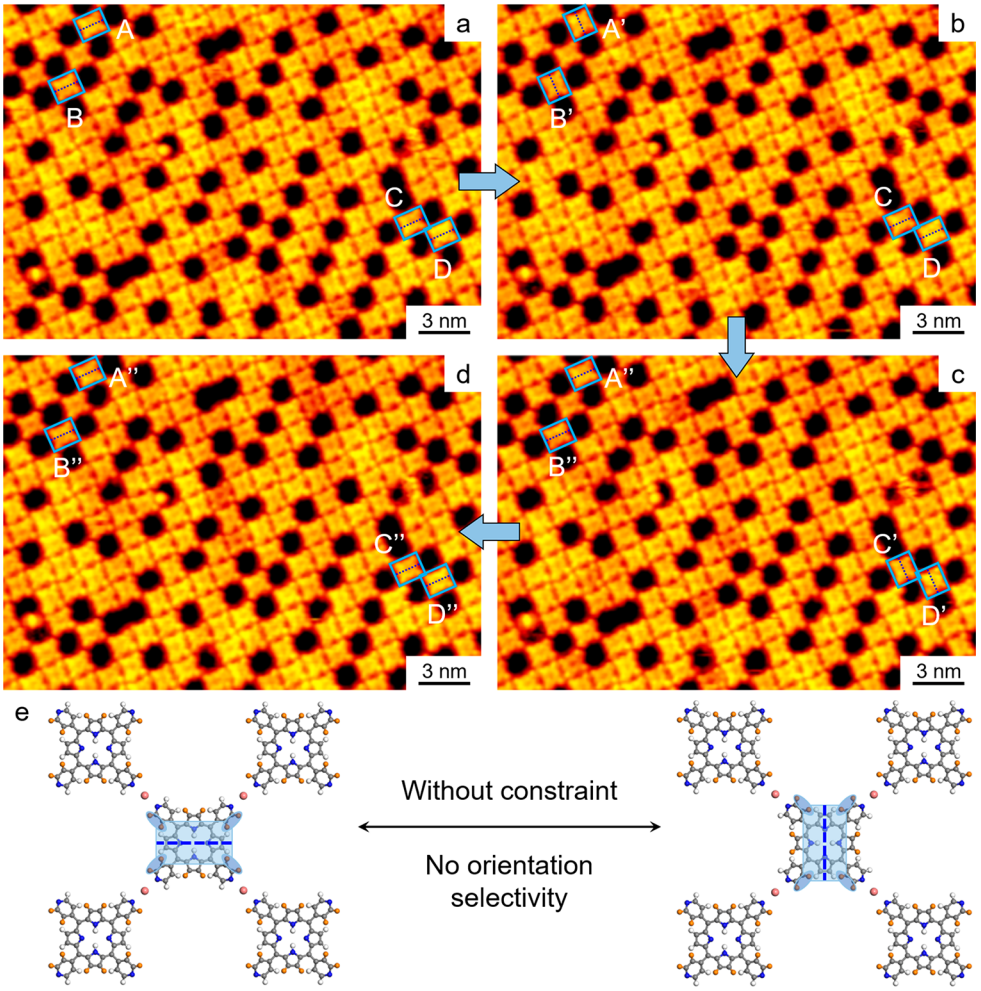

Figure 4. *In situ* interconversion of orientations of molecules with no constraint on any side in a porous network. (a–d) Successive STM images recorded at the same region showing the random interconversion of the two orientations (i.e., transverse and longitudinal) of the molecules (as depicted by blue rectangles and labeled A, B, C, D, respectively) without constraint (i.e., no neighbors interacting on any side) during scanning at RT. Scanning conditions: V_t = −1.2 V, and I_t = 0.6 nA. (e) DFT-optimized structural models of the networks containing the target molecules (shaded blue) with the two orientations on Au(111) (the surfaces have been omitted for clarity), which were calculated to have almost the same potential energy.

As for the orientation change with sufficient space, an isolated molecule adsorbed on Au(111) was applied to simplify the calculations. The energy barriers were calculated to be only ∼0.05 eV for molecular rotation and ∼0.91 eV for conformational change (Figure 5b), indicating that a molecule with sufficient adjacent space would tend to change its orientation via rotation. Interestingly, some asymmetric molecules with a missing leg naturally existed in the chessboard structure, which may serve as marker molecules to speculate the two possible processes experimentally based on the position of the missing part. Accordingly, in large cavities, the marker molecules were manipulated and found to change their orientations by rotation (Figure S10), which is in line with the calculated result.

In addition, to interpret the situation of orientation change with constrained space in a 1D channel, a periodic assembled molecular structure on Au(111) was applied as a simplified system, and two pathways (i.e., molecular rotation and conformational change) were calculated (Figure 5c). Expectedly, the steric hindrance originated from the peripheral molecules significantly modifies the potential energies, and the energy barriers largely increase, which were calculated to be ∼2.01 and ∼1.65 eV for molecular rotation and conformational change, respectively. Note that such a constraint imposed by the local molecular environment also results in a reversed order of the energy barriers of the two possible pathways compared to the case with sufficient space shown in Figure 5b. Thus, an orientation change through a conformational change would be slightly preferred in this situation. While, experimentally, the orientation change of a marker molecule via conformational change or rotation was found to be feasible (see Figure S11 for a detailed discussion).

Furthermore, the last fundamental question is when the orientation change took place, i.e., whether the manipulated molecule changed its orientation before or after diffusion. The calculated pathways in Figure 5c show that after overcoming the energy barrier of ∼1.65 eV to achieve the *in situ* orientation change by conformational change, the next energy barrier for the target molecule to diffuse to the adjacent position is ∼1.08 eV. Accordingly, the conformational change (∼1.65 eV) is the rate-determining step, when the target molecule changes its orientation before diffusion. On the other hand, if the target molecule diffuses to the next vacancy as the first step, it has to overcome the energy barrier of ∼1.72 eV for diffusion and then ∼1.02 eV for the *in situ* orientation change through

https://doi.org/10.1021/jacs.3c03777
J. Am. Chem. Soc. 2023, 145, 22366−22373

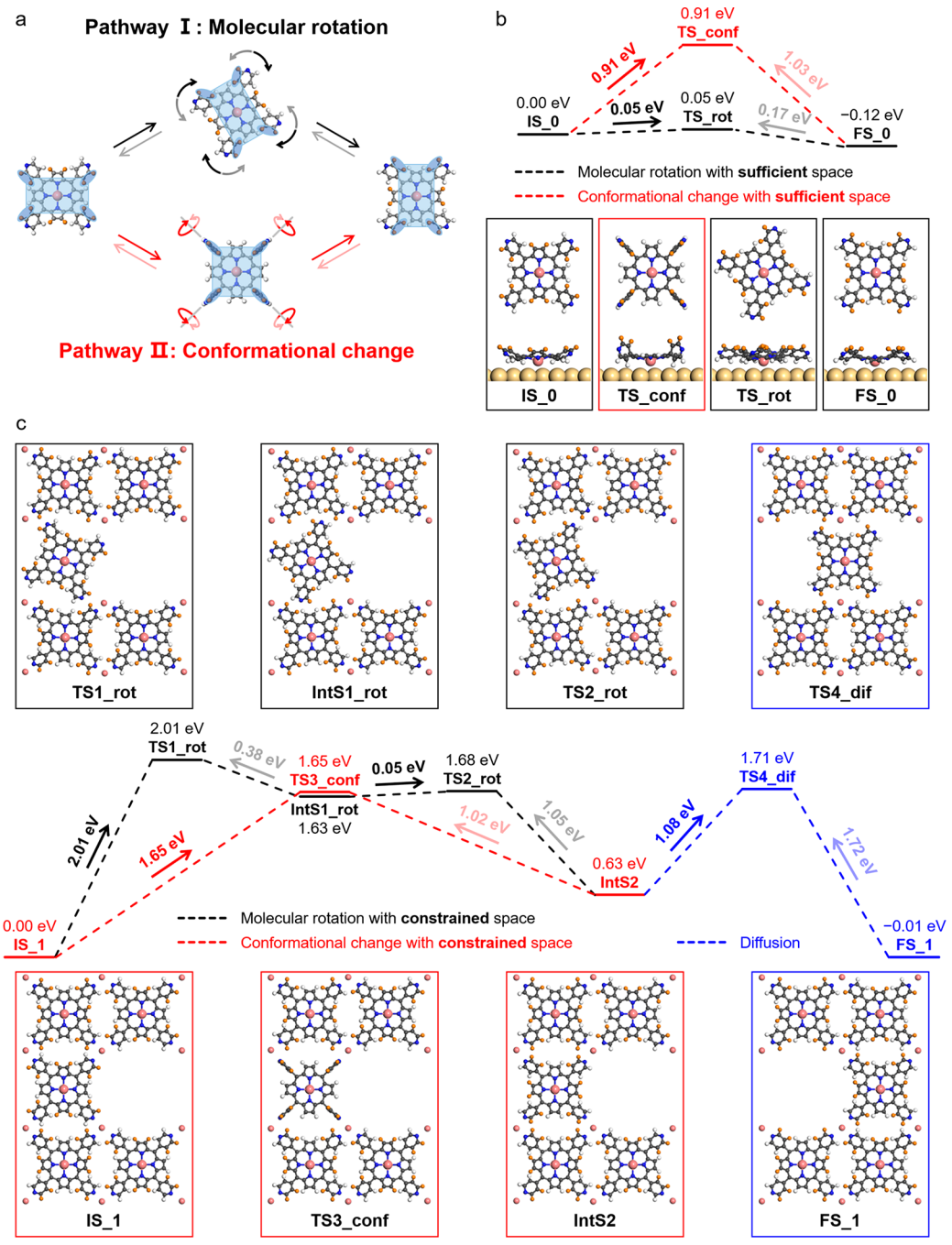

Figure 5. Two possible pathways for the orientation change of a target Na-TPyP molecule in different situations. (a) Schematic illustration showing the orientation interconversion achieved by molecular rotation and conformational change, respectively. (b) DFT-calculated pathways for the orientation change of an isolated Na-TPyP molecule (with sufficient space) adsorbed on Au(111) through molecular rotation and conformational change, respectively. (c) DFT-calculated pathways for the Na-TPyP molecules in the 1D channel (with constrained space) on Au(111) to accomplish the orientation change through molecular rotation or conformational change, followed by diffusion (as depicted by black, red, and blue dashed lines, respectively). The surfaces have been omitted for clarity. The structural models of the initial state (IS), transition state (TS), intermediate state (IntS), and final state (FS) are displayed, and their energies are provided with respect to those of the corresponding IS.

conformational change. In this case, the rate-determining step is diffusion (~1.72 eV). Therefore, due to the similar energy barriers, the "parking" process of a target "sliding-block" molecule may take place independent of the sequence of the orientation change and diffusion.

■ CONCLUSIONS

In summary, by a combination of STM imaging/manipulations and DFT calculations, we report the orientation selectivity of tetrapyridyl-substituted porphyrins constrained in various molecular "Klotski puzzles" constructed from H_2TPyP and NaCl on Au(111). As long as at least one side of a target molecule interacts with an adjacent molecule, a specific orientation (i.e., either transverse or longitudinal) has to be adopted to fit the local molecular environment, where the intermolecular interaction is revealed to be the key to achieving molecular orientation selectivity. It thus provides a way to control specific molecular orientations by predesigning

https://doi.org/10.1021/jacs.3c03777
J. Am. Chem. Soc. 2023, 145, 22366−22373

and constructing the corresponding local molecular environments, i.e., the specific "Klotski puzzles". Our results demonstrate the delicate interplay between molecular orientations and intermolecular interactions in self-assembled structures, which shed light on the fundamental understanding of orientation selectivity and benefit the further development of advanced functional molecular nanodevices.

■ ASSOCIATED CONTENT

Supporting Information

The Supporting Information is available free of charge at https://pubs.acs.org/doi/10.1021/jacs.3c03777.

Methods; supplementary STM images, DFT calculations, and related discussions (PDF)

■ AUTHOR INFORMATION

Corresponding Authors

Wei Xu − *Interdisciplinary Materials Research Center, School of Materials Science and Engineering, Tongji University, Shanghai 201804, People's Republic of China;* orcid.org/0000-0003-0216-794X; Email: xuwei@tongji.edu.cn

Chi Zhang − *Interdisciplinary Materials Research Center, School of Materials Science and Engineering, Tongji University, Shanghai 201804, People's Republic of China;* orcid.org/0000-0002-2335-4579; Email: zhangchi11@tongji.edu.cn

Authors

Zewei Yi − *Interdisciplinary Materials Research Center, School of Materials Science and Engineering, Tongji University, Shanghai 201804, People's Republic of China*

Yuan Guo − *Interdisciplinary Materials Research Center, School of Materials Science and Engineering, Tongji University, Shanghai 201804, People's Republic of China*

Rujia Hou − *Interdisciplinary Materials Research Center, School of Materials Science and Engineering, Tongji University, Shanghai 201804, People's Republic of China*

Zhaoyu Zhang − *Interdisciplinary Materials Research Center, School of Materials Science and Engineering, Tongji University, Shanghai 201804, People's Republic of China*

Yuhong Gao − *Interdisciplinary Materials Research Center, School of Materials Science and Engineering, Tongji University, Shanghai 201804, People's Republic of China*

Complete contact information is available at: https://pubs.acs.org/10.1021/jacs.3c03777

Notes

The authors declare no competing financial interest.

■ ACKNOWLEDGMENTS

The authors acknowledge financial support from the National Natural Science Foundation of China (Grants Nos. 22202153, 22125203, and 21790351), the Fundamental Research Funds for the Central Universities, and Ministry of Science and Technology of the People's Republic of China (2023YFE0101900). The authors are grateful for the use of RIKEN's HOKUSAI supercomputer system.

■ REFERENCES

(1) Yokoyama, D. Molecular Orientation in Small-Molecule Organic Light-Emitting Diodes. *J. Mater. Chem.* **2011**, *21*, 19187−19202.

(2) Chen, W.; Qi, D.; Huang, H.; Gao, X.; Wee, A. T. S. Organic−Organic Heterojunction Interfaces: Effect of Molecular Orientation. *Adv. Funct. Mater.* **2011**, *21*, 410−424.

(3) Hofmann, A.; Schmid, M.; Brütting, W. The Many Facets of Molecular Orientation in Organic Optoelectronics. *Adv. Optical Mater.* **2021**, *9*, 2101004.

(4) Liu, R.; Yang, W.; Xu, W.; Deng, J.; Ding, C.; Guo, Y.; Zheng, L.; Sun, J.; Li, M. Impact of Chemical Design on the Molecular Orientation of Conjugated Donor−Acceptor Polymers for Field-Effect Transistors. *ACS Appl. Polym. Mater.* **2022**, *4*, 2233−2250.

(5) Chen, W.; Huang, H.; Wee, A. T. S. Molecular Orientation Transition of Organic Thin Films on Graphite: the Effect of Intermolecular Electrostatic and Interfacial Dispersion Forces. *Chem. Commun.* **2008**, 4276−4278.

(6) Hou, J.; Yang, J.; Wang, H.; Li, Q.; Zeng, C.; Lin, H.; Bing, W.; Chen, D.; Zhu, Q. Identifying Molecular Orientation of Individual C_{60} on a Si(111)−(7 × 7) Surface. *Phys. Rev. Lett.* **1999**, *83*, 3001−3004.

(7) Otero, R.; Hümmelink, F.; Sato, F.; Legoas, S. B.; Thostrup, P.; Lægsgaard, E.; Stensgaard, I.; Galvão, D. S.; Besenbacher, F. Lock-and-Key Effect in the Surface Diffusion of Large Organic Molecules Probed by STM. *Nat. Mater.* **2004**, *3*, 779−782.

(8) Meng, X.; Möller, J.; Mansouri, M.; Sánchez-Portal, D.; Garcia-Lekue, A.; Weismann, A.; Li, C.; Herges, R.; Berndt, R. Controlling the Spin States of FeTBrPP on Au(111). *ACS Nano* **2023**, *17*, 1268−1274.

(9) Tsukahara, N.; Noto, K.; Ohara, M.; Shiraki, S.; Takagi, N.; Takata, Y.; Miyawaki, J.; Taguchi, M.; Chainani, A.; Shin, S.; Kawai, M. Adsorption-Induced Switching of Magnetic Anisotropy in a Single Iron(II) Phthalocyanine Molecule on an Oxidized Cu(110) Surface. *Phys. Rev. Lett.* **2009**, *102*, 167203.

(10) Cai, Z.; Zheng, L.; Zhang, Y.; Zenobi, R. Molecular-Scale Chemical Imaging of the Orientation of an On-Surface Coordination Complex by Tip-Enhanced Raman Spectroscopy. *J. Am. Chem. Soc.* **2021**, *143*, 12380−12386.

(11) Albrecht, F.; Bischoff, F.; Auwärter, W.; Barth, J. V.; Repp, J. Direct Identification and Determination of Conformational Response in Adsorbed Individual Nonplanar Molecular Species Using Non-contact Atomic Force Microscopy. *Nano Lett.* **2016**, *16*, 7703−7709.

(12) Pavliček, N.; Gross, L. Generation, Manipulation and Characterization of Molecules by Atomic Force Microscopy. *Nat. Rev. Chem.* **2017**, *1*, No. 0005.

(13) Zhong, Q.; Ihle, A.; Ahles, S.; Wegner, H. A.; Schirmeisen, A.; Ebeling, D. Constructing Covalent Organic Nanoarchitectures Molecule by Molecule via Scanning Probe Manipulation. *Nat. Chem.* **2021**, *13*, 1133−1139.

(14) Hla, S. W.; Bartels, L.; Meyer, G.; Rieder, K. H. Inducing All Steps of a Chemical Reaction with the Scanning Tunneling Microscope Tip: Towards Single Molecule Engineering. *Phys. Rev. Lett.* **2000**, *85*, 2777−2780.

(15) Civita, D.; Kolmer, M.; Simpson, G. J.; Li, A.; Hecht, S.; Grill, L. Control of Long-Distance Motion of Single Molecules on a Surface. *Science* **2020**, *370*, 957−960.

(16) Au-Yeung, K. H.; Sarkar, S.; Kühne, T.; Aiboudi, O.; Ryndyk, D. A.; Robles, R.; Lorente, N.; Lissel, F.; Joachim, C.; Moresco, F. A Nanocar and Rotor in One Molecule. *ACS Nano* **2023**, *17*, 3128−3134.

(17) Li, C.; Wang, Z.; Lu, Y.; Liu, X.; Wang, L. Conformation-Based Signal Transfer and Processing at the Single-Molecule Level. *Nat. Nanotechnol.* **2017**, *12*, 1071−1076.

(18) Liu, J.; Li, C.; Liu, X.; Lu, Y.; Xiang, F.; Qiao, X.; Cai, Y.; Wang, Z.; Liu, S.; Wang, L. Positioning and Switching Phthalocyanine Molecules on a Cu(100) Surface at Room Temperature. *ACS Nano* **2014**, *8*, 12734−12740.

(19) Schied, M.; Prezzi, D.; Liu, D.; Kowarik, S.; Jacobson, P. A.; Corni, S.; Tour, J. M.; Grill, L. Chirality-Specific Unidirectional Rotation of Molecular Motors on Cu(111). *ACS Nano* **2023**, *17*, 3958−3965.

(20) Simpson, G. J.; García-López, V.; Boese, D. A.; Tour, J. M.; Grill, L. How to Control Single-Molecule Rotation. *Nat. Commun.* **2019**, *10*, 4631.
(21) Tierney, H. L.; Murphy, C. J.; Jewell, A. D.; Baber, A. E.; Iski, E. V.; Khodaverdian, H. Y.; McGuire, A. F.; Klebanov, N.; Sykes, E. C. H. Experimental Demonstration of a Single-Molecule Electric Motor. *Nat. Nanotechnol.* **2011**, *6*, 625−629.
(22) Manzano, C.; Soe, W. H.; Wong, H. S.; Ample, F.; Gourdon, A.; Chandrasekhar, N.; Joachim, C. Step-by-Step Rotation of a Molecule-Gear Mounted on an Atomic-Scale Axis. *Nat. Mater.* **2009**, *8*, 576−579.
(23) Chiaravalloti, F.; Gross, L.; Rieder, K. H.; Stojkovic, S. M.; Gourdon, A.; Joachim, C.; Moresco, F. A Rack-and-Pinion Device at the Molecular Scale. *Nat. Mater.* **2007**, *6*, 30−33.
(24) Auwärter, W.; Weber-Bargioni, A.; Riemann, A.; Schiffrin, A.; Gröning, O.; Fasel, R.; Barth, J. V. Self-Assembly and Conformation of Tetrapyridyl-Porphyrin Molecules on Ag(111). *J. Chem. Phys.* **2006**, *124*, 194708.
(25) Yi, Z.; Zhang, C.; Zhang, Z.; Hou, R.; Guo, Y.; Xu, W. On-Surface Synthesis of Na-Porphyrins Using NaCl as a Convenient Na Source. *Precis. Chem.* **2023**, *1*, 226−232.
(26) Zhou, K.; Liang, H.; Wang, M.; Xing, S.; Ding, H.; Song, Y.; Wang, Y.; Xu, Q.; He, J.; Zhu, J.; Zhao, W.; Ma, Y.; Shi, Z. Fine-Tuning of Two-Dimensional Metal−Organic Nanostructures via Alkali−Pyridyl Coordination. *Nanoscale Adv.* **2020**, *2*, 2170−2176.
(27) Kong, H.; Wang, L.; Sun, Q.; Zhang, C.; Tan, Q.; Xu, W. Controllable Scission and Seamless Stitching of Metal−Organic Clusters by STM Manipulation. *Angew. Chem., Int. Ed.* **2015**, *54*, 6526−6530.
(28) Xie, L.; Ding, Y.; Li, D.; Zhang, C.; Wu, Y.; Sun, L.; Liu, M.; Qiu, X.; Xu, W. Local Chiral Inversion of Thymine Dimers by Manipulating Single Water Molecules. *J. Am. Chem. Soc.* **2022**, *144*, 5023−5028.
(29) Zhang, C.; Xie, L.; Wang, L.; Kong, H.; Tan, Q.; Xu, W. Atomic-Scale Insight into Tautomeric Recognition, Separation, and Interconversion of Guanine Molecular Networks on Au(111). *J. Am. Chem. Soc.* **2015**, *137*, 11795−11800.
(30) Hou, R.; Guo, Y.; Yi, Z.; Zhang, Z.; Zhang, C.; Xu, W. Construction and Structural Transformation of Metal−Organic Nanostructures Induced by Alkali Metals and Alkali Metal Salts. *J. Phys. Chem. Lett.* **2023**, *14*, 3636−3642.
(31) Eigler, D. M.; Schweizer, E. K. Positioning Single Atoms with a Scanning Tunnelling Microscope. *Nature* **1990**, *344*, 524−526.
(32) Seufert, K.; Auwärter, W.; De Abajo, F. J. G.; Écija, D.; Vijayaraghavan, S.; Joshi, S.; Barth, J. V. Controlled Interaction of Surface Quantum-Well Electronic States. *Nano Lett.* **2013**, *13*, 6130−6135.

https://doi.org/10.1021/jacs.3c03777
J. Am. Chem. Soc. 2023, 145, 22366−22373